Fuel Processing Technology, Volume 163, August 2017, Pages 20 – 34
DOI: 10.1016/j.fuproc.2017.03.030

Burning characteristics of single particles of coal and wood mixtures for co-firing in an upward-flowing hot gas stream

Chinsung Mock[a], Hookyung Lee[b], Sangmin Choi[b], Won Yang[c], Vasilije Manovic[a*]

a* Combustion and CCS Centre, Cranfield University, Cranfield, Bedfordshire MK43 0AL, United Kingdom. Tel.: +44(0)1234 754649; fax: +44 1234751671.

E-mail address: v.manovic@cranfield.ac.uk (V. Manovic)

Burning characteristics of single particles of coal and wood mixtures for co-firing in an upward-flowing hot gas stream

Chinsung Mock[a], Hookyung Lee[b], Sangmin Choi[b], Won Yang[c], Vasilije Manovic[a*]

[a] Centre for Combustion and Carbon Capture and Storage, Cranfield University, Cranfield, Bedfordshire MK43 0AL, United Kingdom

[b] Department of Mechanical Engineering, Korea Advanced Institute of Science and Technology (KAIST), Daehak-ro, Yuseong-gu, Daejeon, South Korea.

[c] Thermochemical Energy System Group, Korea Institute of Industrial Technology, 89 Yangdaegiro-gil, Ipjang-myeon, Seobuk-gu, Cheonan, Chungnam, 31056, Republic of Korea

Corresponding author: V. Manovic, Email: v.manovic@cranfield.ac.uk, Tel: +44(0)1234 754649

Abstract

This study presents the comparative burning behaviours of single solid particles of coal and biomass mixtures for co-firing. In this experimental investigation, a direct observation approach was used to investigate the ignition, flame characteristics and combustion times by means of high-speed photography at 7,000 frames per second. Single particles were entrained into a hot gas stream at 1,340 K and a rapid heating rate at 10^4-10^5 K/s. The apparent volatile flames from the prepared particle size groups were observed within 20-50 milliseconds. To assess the effect of oxygen concentration, particles were burned for their flame characteristics in a range of 10%–40% O_2. The test particles were sieved into three size groups (215–255 μm,

255–300 μm and 300–350 μm) to assess the effect of particle size. Special particles for the co-firing effect were collected individually from two types of mixed pellet: 20:80 and 50:50 coal/wood. Pure sub-bituminous coal and wood particles were also prepared in order to compare their combustion behaviours. In the experimental setup with a cross-injection configuration, sequential combustion processes were effectively and clearly described in terms of particle displacement with time. The experimental results showed distinguishable flame characteristics from single particles of coal, 50:50 coal/wood, 20:80 coal/wood and wood, including soot flame size and intensity. The impact of high coal-blending ratio caused an increase in the flame size and intensity and the ignition time was close to that of pure coal particles. Quantitative measurements of combustion events on co-firing particles were also discussed in relation to significant impacts of the particle size and the oxygen concentration.

1. INTRODUCTION

Co-firing is a promising technique with several benefits, the most important of which are environmental ones. Simultaneous burning of coal and biomass emits low NET carbon dioxide [1, 2] and the sulphur oxide (SO_x) and nitrogen oxide (NO_x) emissions from this combustion are generally lower, compared with the coal-fired combustion [3–6]. The economic benefits of this type of combustion are fuel price stabilisation, fuel flexibility and low-risk costs of retrofitting coal-fired plants with fuel-blending control systems for biomass particles [7, 8]. The main challenges with co-firing come from the characteristics of biomass particles in relation to chemical composition, fibrous shape and relatively large particles (~3 millimetres for biomass, ~150 μm for coal in p.f. boiler) [9, 10] with relatively low energy density [11, 12]. Their irregular shape and wide particle size range during combustion play a significant role in burning behaviours such as ignition, volatile flame and char combustion [13]. The significant differences between biomass and coal are the wide disparity in volatility and the fixed carbon content of different types of biomass. The volatile matter content of biomass is greater than that of coal and the fixed carbon content is less, which contributes to their different burning behaviours regarding volatiles and char combustions [14–16]. From a previous study [17], pulverised biomass particles are known to exhibit flame characteristics that are associated with a small flame and low intensity during homogeneous combustion. Besides, the volatile matter in biomass is released earlier than that in coal because of the different ignition temperatures of their organic compositions [18–20]. Consequently, the burning behaviour in co-firing is attributed mainly to the biomass type and its mixtures.

Soot loading in volatile flames plays an important role in generating radiation heat transfer, because of soot luminosity, as illustrated by the equation: $q_{radiation}=\varepsilon 4\sigma T^4 \Delta t$, where $\varepsilon=1-(1+kf_vLT/c_2)^{-4}$ [21, 22]. There have been studies on average soot volume fraction from

different types of coal [15]. It is believed that biomass has less flame luminosity, where gas is the major phase in the flame. Atiku et al. [24] measured soot particles, which consist of elemental carbon (EC) and organic carbon (OC), between biomass and coal. During flaming combustion, eight times as much elemental carbon was collected from burning coal. In the experiment, the apparent volatile flame would be discussed for comparative soot intensity between co-firing particles and pure solid particles.

An in-depth understanding of the thermal decomposition and combustion in co-firing would certainly be beneficial. Several studies [2, 7, 18–20, 24–28] have reviewed technical considerations and conducted biomass combustion with coal in extended experimental investigations. In thermogravimetric analysis (TGA), the devolatilisation of biomass–coal has been investigated extensively at low heating rates, with focus on the ignition characteristics [18], kinetic analysis [19] and primary reactions [25]. However, the experimental results of such studies have not been adequately explained in the context of practical combustion behaviour. This is because the actual pulverised solid-fuel particles in power plants are generally burned rapidly and are accompanied by complicated reactions and events. Gani et al. [26] investigated the co-combustion of coal with biomass in relation to ignition, NO_x emission and ash formation in a drop-tube furnace at 800°C. They plotted the temperature profile along the furnace during biomass, coal and co-combustion and showed that co-combustion yields the highest temperature of the three. Lu et al. [27] reported that adding biomass can prolong ignition in co-firing because of the large particles and high moisture content of the biomass. They also investigated flame characteristics such as brightness, temperature and ignition in industrial-scale coal combustion. However, there were uncertainties such as the loading of particles, their sizes and environmental conditions; these limited the extent to which they were able to explain the flame parameters. Therefore, for a

comparative analysis to clarify the combustion behaviour of solid-fuel particles with clearly defined physical properties under well-controlled conditions, it is necessary to burn one particle at a time.

In previous studies [17, 29], we investigated the combustion of single coal and biomass particles in a lab-scale entrained-flow reactor. The experiments were carried out under rapid heating rates and a high gas temperature in order to describe the particle combustion process and investigate the flame characteristics. Khatami, Levendis et al. [30–32] also observed the behaviour of single particles of individual coal and biomass in a drop-tube furnace. However, the observations of flame structure from these experiments are neither fully understood nor explained in relation to co-firing. Different physical and chemical events can occur in co-firing because of a mixture of solid fuel particles. Unfortunately, no experimental research has been reported on single particles of pulverised coal and biomass mixtures.

This paper reports an investigation of burning single particles, which were produced from a mixture of pulverised coal and biomass, using direct observation. Sequential combustion processes such as heat-up, devolatilisation and char combustion are described in detail. The effects of having single particles with different blending ratios, sizes and oxygen concentrations are also discussed. Given the statistical uncertainties related to single particles of homogenous fuel mixtures (20:80 and 50:50 mixtures of coal and wood), there was a clear need for particle definition from sub-experiments such as scanning electron microscopy (SEM), fuel properties and TGA, prior to the main experiment. The experimental results are compared to discuss their ignition and combustion time and flame parameters with pure wood and coal single particle burning behaviours through quantitative analysis.

2. METHODOLOGY

2.1 Experimental apparatus

The experimental combustion study of solid fuel particles was performed in a lab-scale entrained-flow reactor as shown in Fig. 1 with optical access to the burning single particles. The square-shaped quartz tube is 45 mm in length and width and 800 mm in height, and a honeycomb burner is located at the bottom for an upward flow of post-combustion gas. An electrical guard heater shields the quartz to minimise the temperature drop of the post-combustion gas except across the optical access section. Particles are injected at ambient temperature (298 K) via a water-cooled injector made of stainless steel double tubes: an outer tube for cooling water and an inner tube for the carrier gas and particles. This injector is positioned above a porous flow straightener in the cross-flow configuration in which single particles are entrained from the horizontal cold carrier gas into the vertical hot gas stream. The injector is also placed 20 mm from the interior wall to minimise temperature and flow differences between the hot gas stream and the wall. To support the temperature environment, the temperature gradient in the optical access section is shown in Fig. 1 by a simulation image (Fluent 13.0) that includes a prediction of particle displacement during burning. The carrier-gas flow rate is 0.5 slpm in all experiments and the particles are injected at 25–30 particles/min by a micro-syringe injector.

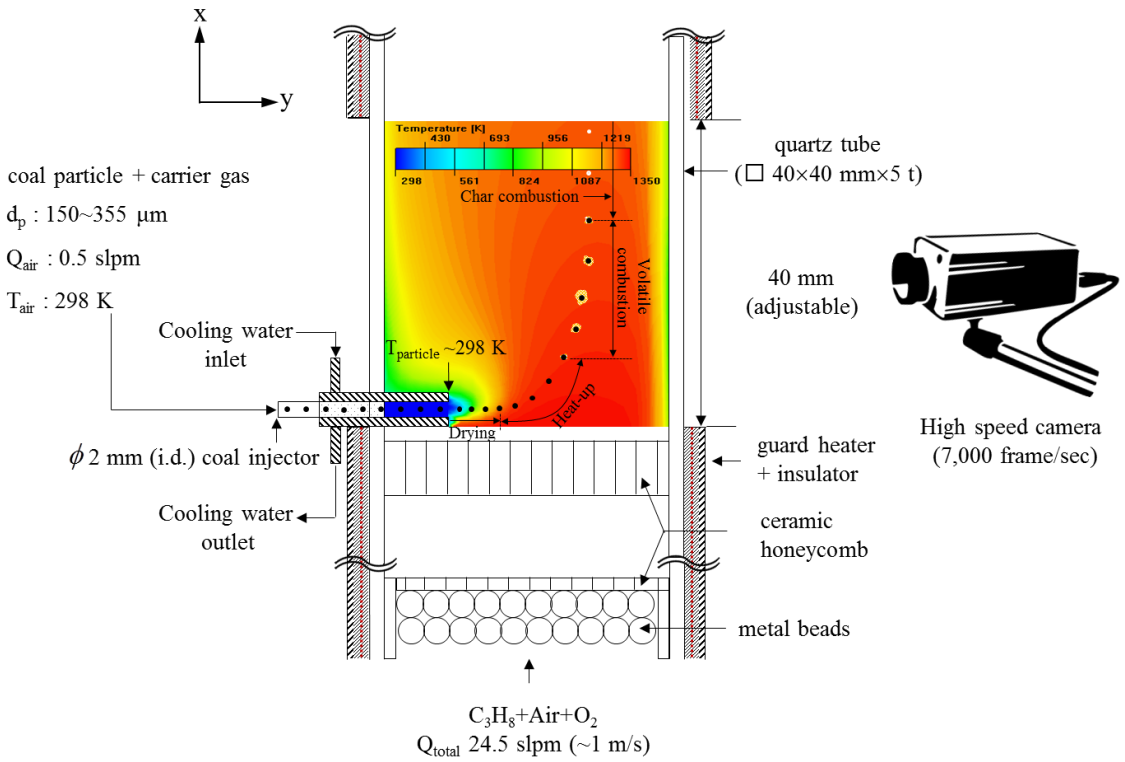

154

155 Fig. 1. Schematic diagram of the lab-scale entrained-flow reactor for a few hundred micron-
156 sized single solid particles. Also shown are the temperature fields of the hot gas stream (red)
157 and cold carrier gas (blue), which explain the temperature gradient and the predicted
158 sequential combustion processes of burning particle in the optical access section.

159 **2.2 Environmental conditions**

160 The variable-supply gas inputs of C_3H_8, O_2 and air into the honeycomb are controlled for
161 10%–40% oxygen concentration, whereas the flow rate of these gases is maintained
162 identically at 24.5 slpm for the experiments. The following main flue gases are produced: N_2
163 (38.2%–67.9%), O_2 (10.4%–40.1%), H_2O (12.4%) and CO_2 (9.3%).

164 The gas temperatures were measured on the basis of radiation loss of the probe of an R-type
165 thermocouple at 21 locations in x- and y-axis: 0, 7, 14, 21 and 50 mm from the injector along
166 the y-axis and 2, 19, 20, 30 and 39 mm along the x-axis. To obtain a mean value, temperature

was averaged over 30 seconds. The variation in adiabatic flame temperatures from the post-combustion was approximately 140 K from 10 % to 40 % oxygen concentration. The mixing zone of the leftward-flowing cold carrier gas and the upward-flowing hot main gas stream is shown in Fig. 2. As particles pass through this zone, their temperature increases up to the devolatilisation or ignition temperature. The highly interacting flow zone at 0 mm along the *y*-axis is also sufficient to affect particle motion and combustion. Khatami et al. [31] discussed the change in combustion behaviour of a particle between quiescent gas conditions (no flow) and active gas flow. Therefore, the environment with the mixing zone and cross injection configuration enables an exclusive description of sequential combustion processes such as drying, heat-up and volatile combustion regimes that accompany particle motion.

The velocities of post-combustion gas and cold carrier gas in a cross-jet apparatus have been discussed by Lee et al. [33]. The particle velocities during the release of volatile matter vary according to these physical quantities, so all experiments were performed under identical vertical and horizontal velocities: ~1 m/s for the post-combustion gas and 2.5 m/s for the cold carrier gas.

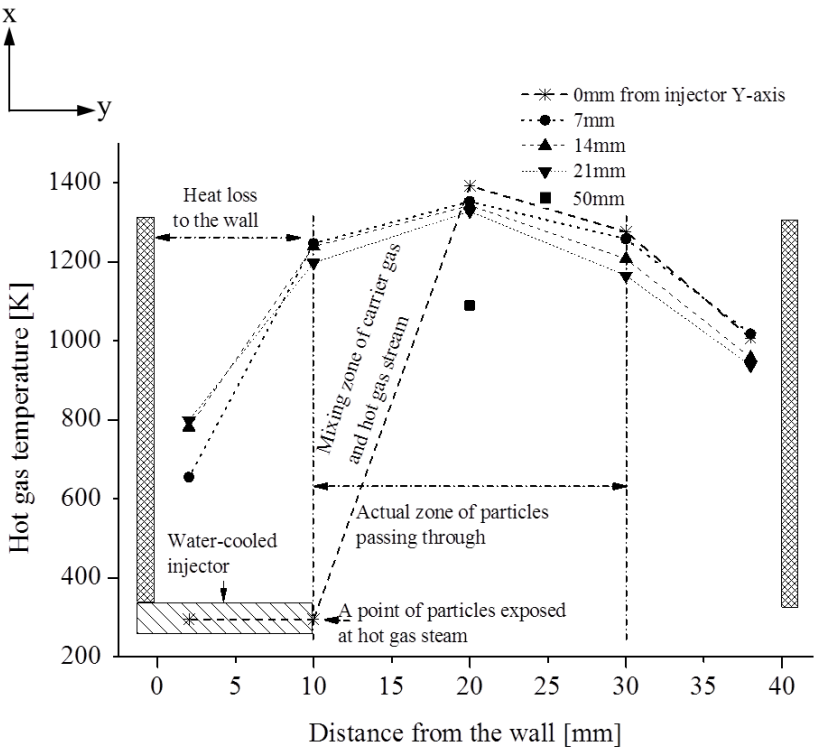

Fig. 2. Experimental measurements of surrounding gas temperatures in the optical access section. This shows the actual zonal temperatures of particles passing through and the predicted initial particle temperature before heat-up.

2.3 Particle properties

The coal used in this study was a sub-bituminous type mined by Adaro Energy in Indonesia; the biomass was pine wood logged in Gyeongsang Province, South Korea. These materials were used for making a few-hundred-micron-sized single particles with a coal-to-wood fuel ratio of either 50:50 or 20:80. To produce these special particles, we first created pellets in a pellet factory through a sequence of pulverising and sieving the raw coal and wood (step 1), mixing the resulting powders (step 2) and compressing the mixture into pellets (step 3), as shown in Fig. 3. In step 1, particles are milled separately by species and sieved to under 100 μm; anything larger can spoil a homogeneous mixture. Step 2 is an initial fuel mixing process in which the same volume (500 mL) of coal and wood or 200 mL and 800 mL,

196 respectively, are added to a container before being shaken and then sieved for 20 min. The
197 final step is the pelletizing process, which involves another mixing process with the addition
198 of 2 kg of water per 1 m^2 of particles. This water content plays an important role in the
199 physical bonding of different solid fuel particles as an adhesive source; this particular level of
200 water loading was determined through repeated tests of pellet stability/integrity.

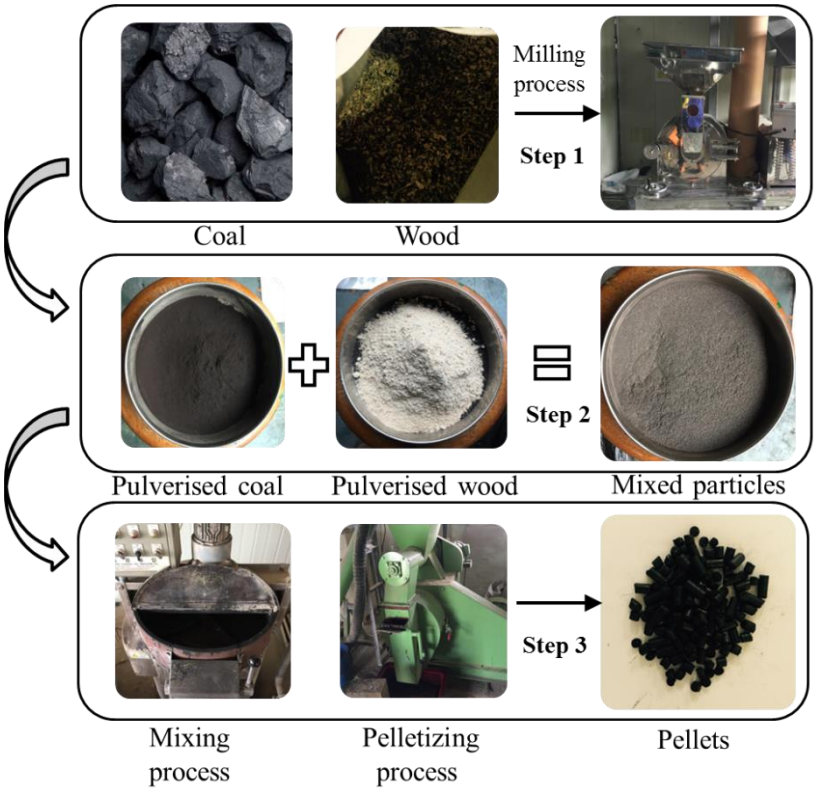

201

202 Fig. 3. Preparation of pellets with 50:50 or 20:80 coal/wood mixtures. This figure shows how
203 the pellets were made with fuel blending for co-firing, prior to being pulverised into a few-
204 hundred-micron-sized particles.

205 Two types of pulverised co-firing particles were obtained from several separation methods
206 that have been described in detail previously [17]. Some of the collected particles inevitably

have irregular shapes with high aspect ratio because of the fibrous wood particle structure, but these can be separated using an inclined plane. The particles were separated into size groups (215–255 μm, 255–300 μm and 300–355 μm) using seven testing sieves with different mesh diameters: 215, 255, 300 and 355 μm. Repeated tests with uncoated paper on an inclined plane allowed the particles to be sorted by shape, e.g., flat, cylindrical, or spherical. In the experiment, only the spherical-like shape is used because the cross-jet injection is limited in burning irregular particle shapes. Flat-like and cylindrical-like particles lead to very random trajectories with non-uniform particle motion in the reactor.

Four particles were subjected to chemical composition analysis on an as-received basis, as shown in Table 1. These analysis data were obtained using the thermogravimetric analyser (TGA-701) at the Energy and Environment Research Centre of the Korea Advanced Institute of Science and Technology (KAIST). The changes in volatile matter and fixed carbon mass fraction for the 50:50 blended particle were approximately +15% and −16.6%, respectively, compared with coal particles, whereas for the 20:80 blended particle they are +26.7% and −27.7%, respectively. The blended particles have higher moisture content because of the water added during pelletising. However, the moisture differences between the four particles after the pulverising process are too small to noticeably affect their combustion behaviours.

The bulk densities of the four particles were measured using a simplified bulk density technique that involved filling a bottle with pulverised particles. This method allows the density of each packed-bed particle to be calculated based on $\rho_p = (m_{b,p}–m_{b,e})/V_{b,w}$, where ρ_p is the particle density, $m_{b,p}$ is the mass of the bottle filled with particles, $m_{b,e}$ is the mass of the empty bottle and $V_{b,w}$ is the volume of the bottle determined from water filling. Using coal for the reference bulk density, the relative bulk densities of 50:50 coal/wood, 20:80 coal/wood and wood are 570 kg/m^3, 430 kg/m^3 and 340 kg/m^3, respectively. From measuring

these particle densities, the energy densities were calculated as 19.581 GJ/m^3 for coal, 12.490 GJ/m^3 for 50:50 coal/wood, 8.530 GJ/m^3 for 20:80 coal/wood and 6.215 GJ/m^3 for wood.

The difference in chemical composition between coal and wood particles is shown in Fig. 4 in a Van Krevelen diagram that indicates the relationship between the hydrogen/carbon (H/C) and oxygen/carbon (O/C) ratios. Coal particles have the lowest H/C (0.73) and O/C (0.28) ratios, whereas wood particles have the highest H/C (1.34) and O/C (0.89) ratios. The latter contain highly volatile matter that is high in oxygen and low in fixed carbon. The presence of high oxygen content plays a significant role in the reactivity of the pyrolysis, and the tar yield is proportional to the H/C ratio [34].

Table 1. Chemical compositions of four samples

Sample	Proximate analysis (wt. % ar)[1]				Ultimate analysis (wt. % daf)[2]					LHV[3&1] (MJ/kg)	Particle bulk density (kg/m^3)	Approx. energy density (GJ/m^3)
	V.M	F.C	Ash	M	C	H	O	N	S			
Coal	42.0	46.1	1.5	10.4	64.4	4.7	18.1	0.9	0.1	25.43	770	19.581
Coal-Wood (50:50 %)	57.0	29.5	1.3	13.0	58.6	6.2	28.1	0.6	0.1	20.82	570	12.457
Coal-Wood (20:80 %)	68.7	18.4	0.6	11.7	52.3	6.4	35.4	0.4	0.1	17.14	430	8.530
Wood	81.5	9.7	0.1	8.5	48.5	6.5	43.2	0.2	0.1	25.43	340	6.215

[1]as received [2]dry, ash free [3]lower heating value

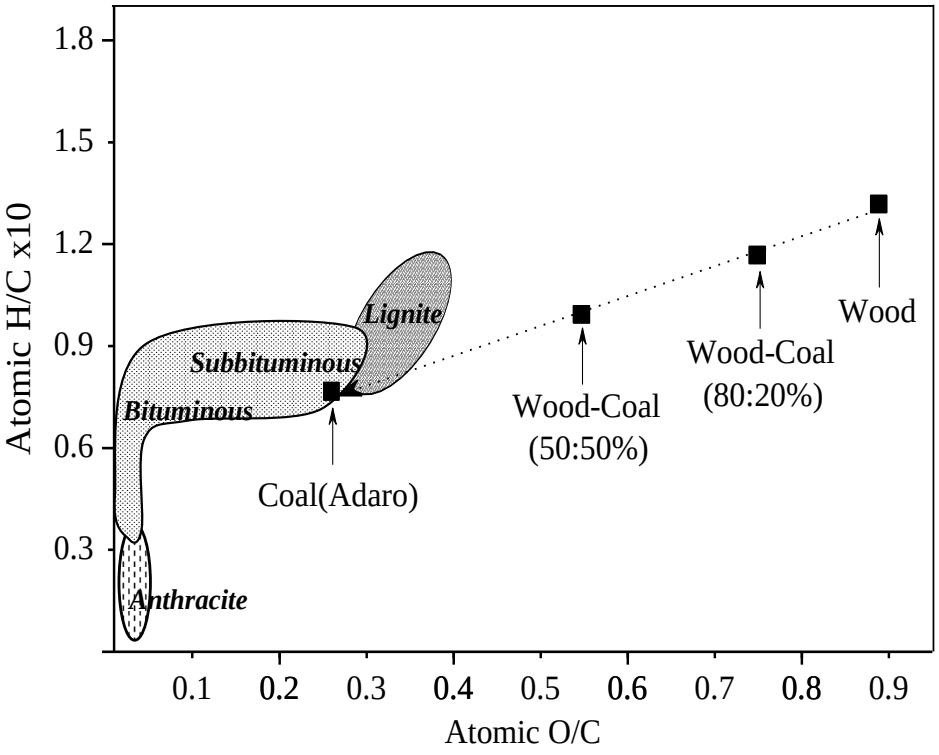

Fig. 4. Van Krevelen diagram for the four different solid fuel particles.

2.4 Direct observation of burning particles

A high-speed camera (Phantom V710) was used for direct observation of the burning particles. It can record at 7,000 frames per second and is fitted with a micro-lens (Nikon Micro-NIKKOR 105 mm f/2.8) as shown in Fig. 5. The magnification of the microscope lens was determined through repeated tests with 30-mm and 200-mm micro-lenses to record clear images of the soot flame in the maximum range of combustion regimes. The complementary metal oxide semiconductor (CMOS) image sensor in the camera was 25.6 mm × 16.0 mm and a resolution of 1,280 × 800 pixels was selected to provide a quantitative analysis of the burning particles. Lee et al. [29] introduced the calibration method with minimal observation errors wherein the pixel size was calibrated using circle and line-scale reticle shapes, fitted inside the field of view of the camera. Without a backlight, the flame intensity on a particle's

surface was too bright to allow char particles to be captured simultaneously. The flame intensity varied according to the type of solid particle; for example, a coal particle burns with almost twice the intensity of a biomass particle [17]. Therefore, determining the backlight intensity played an important role in comparing the flame structures of the four particles. A controllable-brightness, light-emitting diode (LED) backlight with uniform luminescence and high intensity was adapted identically at 5,600 K for all experiments and was located at 50 mm from the quartz window.

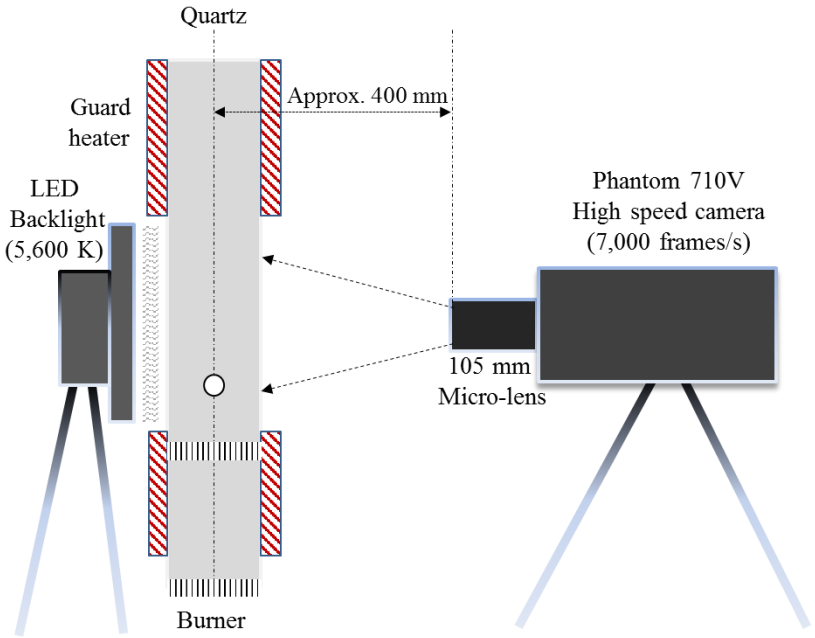

Fig. 5. Configuration of the high-speed camera and LED backlight. This enables the observation of particle ignition and volatile and char combustion on the few-hundred-micron-sized surfaces.

2.5 Physical formation of the four particles from SEM images

To explain the particle structures of the fuel mixtures, pulverised particles were examined using a NOVA 230 SEM. The resulting images shown in Fig. 6 were taken under the

following conditions: accelerating voltage 10.0 kV, spot size 3.0, magnification 650–800×. The pure wood and coal particles were compared with the two co-firing particles. First, the raw wood particle had a remarkably fibrous structure with a high aspect ratio, and the external physical structure of the coal particle was an irregular blocky shape with angular transitions. These appreciably different shapes can play an important role in particle motion, temperature gradient and ignition [33, 35].

They may also exert a strong influence on differences in combustion behaviour, such as flame structure, release of volatile matter and combustion mode. The blended particles were physical mixtures of coal and wood fragments, and the small coal particles could appear inside or on the particles. The fuel blending ratios (50:50 or 20:80) were fairly constant according to the volume fractions of coal particles used in the pelletising process. However, it is difficult to guarantee a homogeneous mixture of pulverised particles. Repeated tests showed remarkable differences in the apparent flame structures of each particle group but similar combustion behaviour in identical particle groups. The standard deviation was less than 10% in all experiments. We analysed the thermal decomposition of the four particles to support whether the particle mixtures were homogeneous or not, as discussed later in section 3.

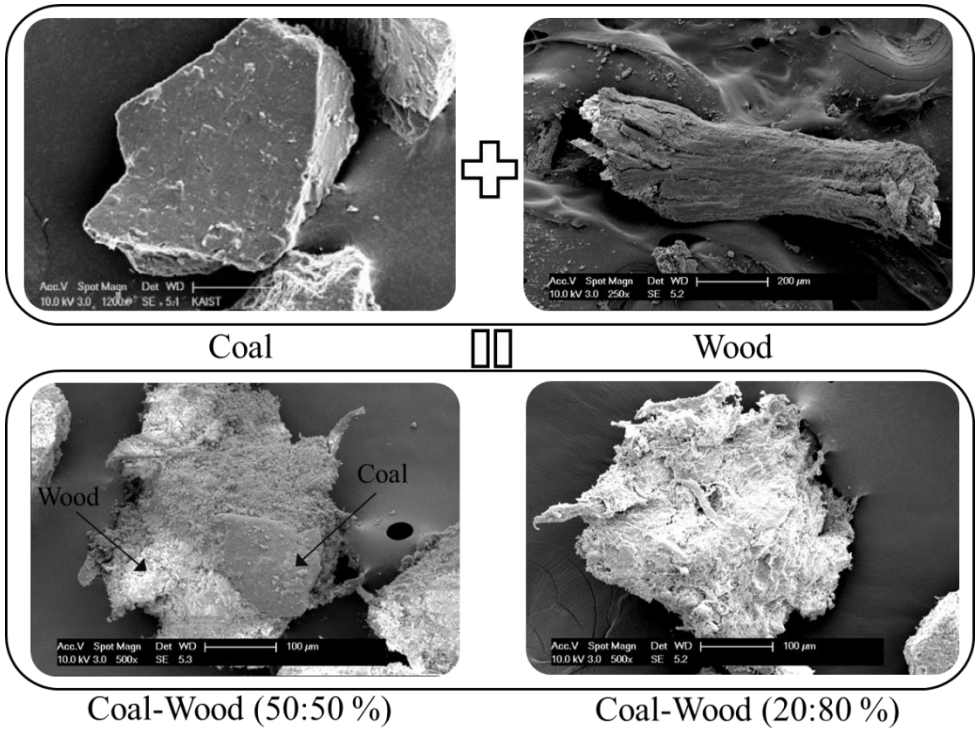

Fig. 6. SEM images of coal, wood, 50:50 coal/wood and 20:80 coal/wood particles.

2.6 Characterisation of volatile flame on pulverised coal and raw wood particles

Flames comprise pyrolysis and luminous regions in which a gas phase and a solid phase (as submicron soot particles) are released by the chemical reactions. The luminous region is occupied in a flame and the high radiative energy is generated mostly from the soot particle fraction. The fixed carbon content plays an important role in the formation of an elongated soot cloud, because this content is equivalent to elemental carbon, which is one of the elements that produce soot particles [36]. Here we discuss the physical appearance of flames due to coal and wood particles prior to the investigation of single particles with different fuel mixtures. As shown in Fig. 7, the different size and shape in volatile flames for both sub-bituminous coal and wood particles at 1,340 K were observed under 10-40 % O_2. The diffusion flame of coal was found to be several times larger than the wood flame under all

oxygen concentrations. Increasing the coal particle size under low O_2 concentration enhanced the elongated flame. This result is consistent with previous research [29, 37]. The attached flame is formed where the rate of volatile release is balanced by the rate of oxidation, but this fast oxidation rate decreases the radius of the volatile flame and enhances the detached flame depending on biomass species, particle size and particle heating rates. Especially, biomass particles have thin volatile flames under high oxygen concentration because of their turbulent dispersion of gas-phase, which is the major species in a flame. Coal particles under low O_2 concentration have an elongated flame with a soot tail. This tail is formed by the effect of thermophoresis (force and velocity) between the solid phase and surrounding gas and low availability of oxygen [38–40]. The differences in this soot tail are less pronounced at higher oxygen concentration [41].

The flame characteristics of pure coal and wood particles offer a meaningful comparison for the flame parameters of the two co-firing particles with different fuel-blending ratios. In the experimental results, the intensities of volatile flames for the four particles were analysed by image processing, which converts a flame image into a grayscale image. In the process, each pixel in the image has different values in a range of 0 to 255, and numerical background values, which were more or less than 65, are extracted from the images. After that, the intensity of the flame was divided by the maximum value of grayscale (255). The intensity-weighted values in the flame boundaries were fluctuating, which means that it might be considered a flame threshold. To minimise their fluctuation and verify the minimised variation of the flame size, we have carried out the sensitivity analysis with varying back-lighting intensity until the rate of change in the flame size was minimised.

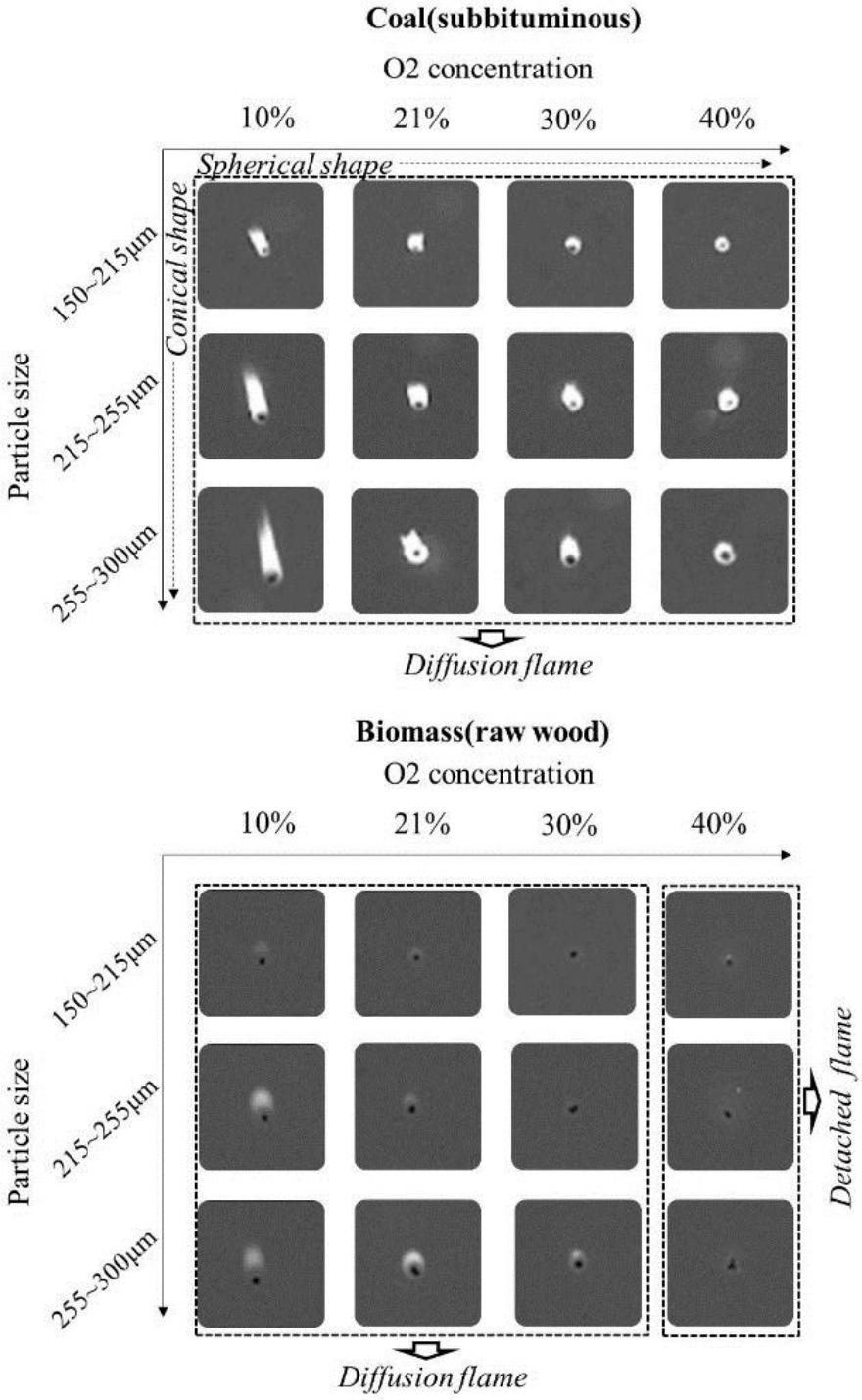

Fig. 7. Typical flame structures of pure coal and wood in relation to shape and size under 10–40% O_2 and at 1,340 K. This illustrates the physical changes due to particle size and O_2 concentration, and explains the corresponding volatile combustion modes of attached,

diffusion and detached flames.

3. RESULTS AND DISCUSSION

3.1 Sequential combustion processes under slow heating and thermal decomposition for different fuel-blending ratios

It is generally accepted that the impact of co-firing sub-bituminous coal (Adaro) with biomass (pine wood) contributes to rapid devolatilisation, fast ignition and low emission of carbon dioxide because of the chemical and physical characteristics of wood. Thermogravimetric analysis, TG/DTA 92-18, was used to investigate the characteristics of co-firing particles with different fuel blending ratios compared to raw wood particles. Each sample was prepared at 8±0.5 mg from pulverised particles in the range of 150–215 μm, and the samples were heated at 20 K/min to 1,273 K under air conditions. The results explained the thermal decomposition and how the mass of these samples reduces differently as a function of temperature over time. The main experiment was carried out under rapid heating, but the TGA here was done under slow heating that is not representative of practical conditions in an industrial furnace. In spite of this limitation, the different thermal decompositions of 20:80 and 50:50 coal/wood and wood particles can be discussed in relation to the impact of co-firing combustion and by comparing the combustion behaviour with that under rapid heating rate. Thermogravimetric (TG) plots and derivative thermogravimetric (DTG) curves, which are obtained from the derivatives of the TG profiles, are shown in Fig. 8. The results show unequal TG and DTG curves, with the first and second peaks of mass reduction followed by fluctuations between 50:50 coal/wood, 20:80 coal/wood and raw wood. In relation to the combustion processes, the first peak is due to the drying process that occurs at 300–400 K, after which the particle is heated up with negligible mass reduction. Sequentially, the volatile release starts at approximately 520 K and the peak reaches almost

610 K because pure wood particles have three components: lignin, cellulose and hemicellulose**.** A fluctuation then occurs because of lignin decomposition. Generally, hemicellulose decomposes in a range of 493–588 K, cellulose does so at 588–673 K and lignin does so over a wide range of 433–1173 K [42]. Finally, the particle mass decreases at constant mass loss rate, which is associated with char combustion. The second peak and degree of fluctuation magnitude were obviously different between the three particles, which is attributed to either the volume of wood particles or the volatile mass fraction in a particle. Coal particles have a moderate peak and the char combustion regimes are extended because of their high carbon content. Consequently, under slow heating, the highest peak for devolatilisation occurs for the raw wood particle, and the co-firing particles also have higher peaks at relatively low temperatures. However, the flame ignition and combustion behaviours under this slow heating rate does not correspond with those of a single burning particle under rapid heating rate. This aspect is discussed in section 3.2.

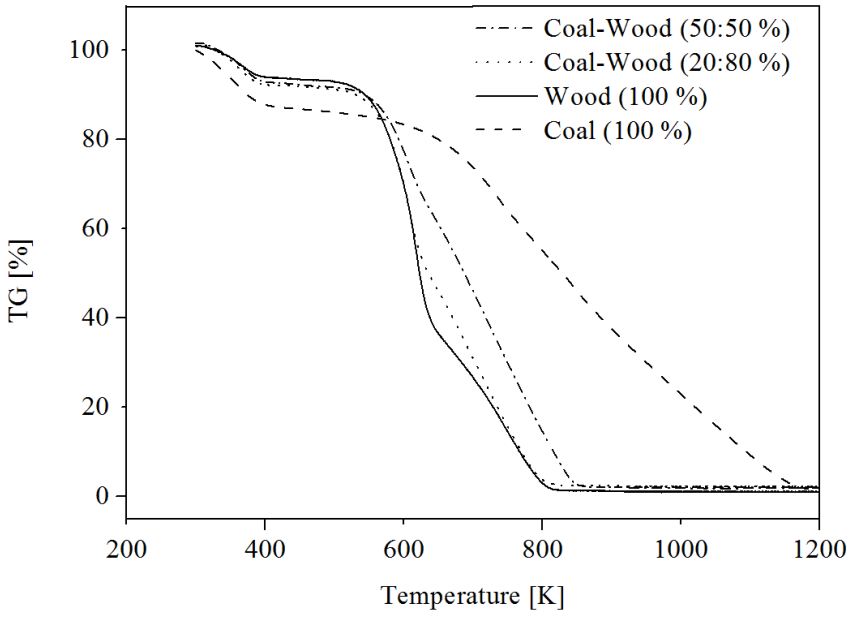

(a)

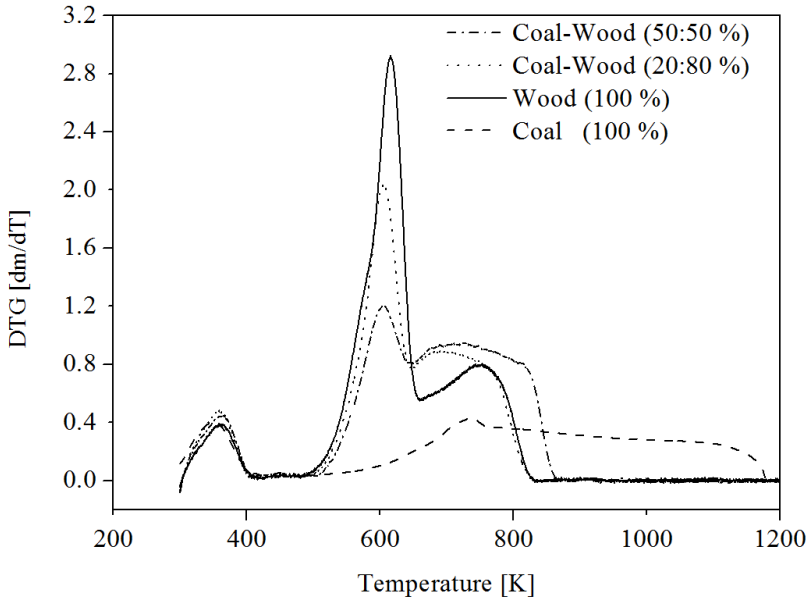

(b)

Fig. 8. Thermal decompositions of 50:50 coal/wood, 20:80 coal/wood and pure wood obtained from TGA at a heating rate of 20 K/min: (a) TG, (b) DTG. These graphs explain the distinction between mass reduction associated with homogeneous and heterogeneous combustion between the two prepared co-firing particles, coal particles and pulverised wood particles.

3.2 Sequential combustion processes under rapid heating and development of volatile flames for different blending ratios

The sequential combustion processes of a pulverised solid-fuel particle are explained in the superimposed images in Fig. 9. Single particles of coal, 50:50 coal/wood, 20:80 coal/wood and wood in size ranges of 215–255 μm and 300–355 μm were burned under 10% oxygen concentration and at 1,340 K. Particles are heated rapidly by the drying process after particle injection at 298 K. The release of volatiles then starts within a few milliseconds, followed by volatile combustion. Char combustion starts after extinction of the volatile flame, but this

389 regime is not shown because of limited optical access. Under rapid heating rates, volatile
390 combustion presents changes in the flame size, following volatile ignition. Comparative
391 flame size and intensity with sequential combustion processes can be explained as a function
392 of time. In contrast, TGA, which is operated under slow heating rates, shows the fluctuated
393 profile with a peak for the regime of volatile combustion, providing a range of particle
394 temperature for volatile and char combustion and a different rate of devolatilisation between
395 the four particles. The similar tendency of volatile combustion was shown in the results, but
396 there are more complex physical and chemical events in a flame around a particle under rapid
397 heating. Generally, high soot formation in a flame is associated with tar reacting to become
398 submicron-sized soot particles at high temperatures. This affects the volatile combustion
399 associated with highly luminous flames [43, 44]. From this result, the four burning particles
400 differed in apparent homogeneous ignition and apparent flame structures. The pure coal
401 particle (215–255 μm) ignited after 30 ms, whereas the wood particle ignited after 48 ms. The
402 single particles with fuel mixtures ignite in almost the same way as does the coal particle,
403 which is attributed to the coal ignition characteristics. To see this in more detail, the results
404 for ignition and combustion times are discussed in Fig. 12–15, where it can be seen that
405 increasing the coal blending ratio has an impact on large elongated flames with their high
406 intensity.

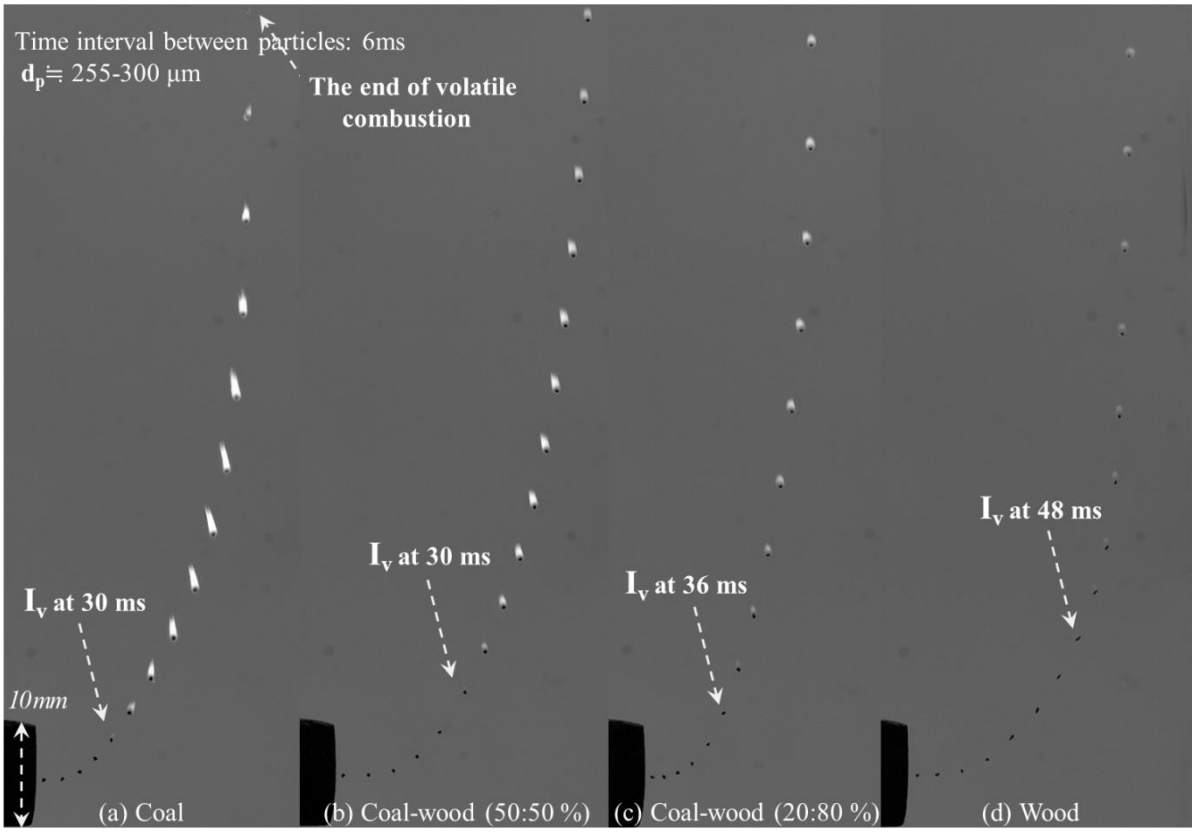

Fig. 9. Sequential combustion-process images of four solid particles ($d_{255–300\ \mu m}$, T_g = 1340 K and 10% O_2 concentration). After leaving the tip of the injector, each single particle is marked at intervals of 6 ms as it forms an apparent volatile flame from initial ignition.

3.3 Ignition delay, volatile combustion time and flame characteristics

Figure 10 shows the average heat-up (or ignition) and volatile combustion durations for the four particles from 20 of each particle under different oxygen concentrations at 1,340 K. The standard deviation of each test is less than 10% of the mean values from the quantitative analysis. The heat-up time is measured from when the particle is injected until the apparent volatile ignition. This ignition might be different from homologous ignition, because a light gas phase emits a very weak light. Therefore, this experiment presents only the apparent volatile ignition with soot luminosity. The results show that, under 10% oxygen, the coal particle and the two co-firing particles have shorter ignition delays (26–30 ms) than that of

421 the wood particle (40 ms).

422 Under all oxygen levels, the differences in apparent volatile ignition between particles
423 (except for the pure wood particles) are not significant because of early ignition, based on
424 apparent volatile ignition of the coal particle. The volatile combustion time of the co-firing
425 particles is almost the same as that of wood. In other words, the different ignition and volatile
426 combustion times of the co-firing particles can be attributed to both coal and wood,
427 respectively.

428 The apparent flame characteristics of the four particles at 215–255 μm are explained under
429 10, 21 and 30% O_2 as shown in Fig. 11. Overall, the size of the volatile flames decreases with
430 the shorter combustion time as the oxygen concentration increases. This result shows that the
431 four particles have distinguishable flame structures in terms of size and intensity under all
432 oxygen levels. Their flame size and intensity are explained by a quantitative analysis in
433 section 3.4.

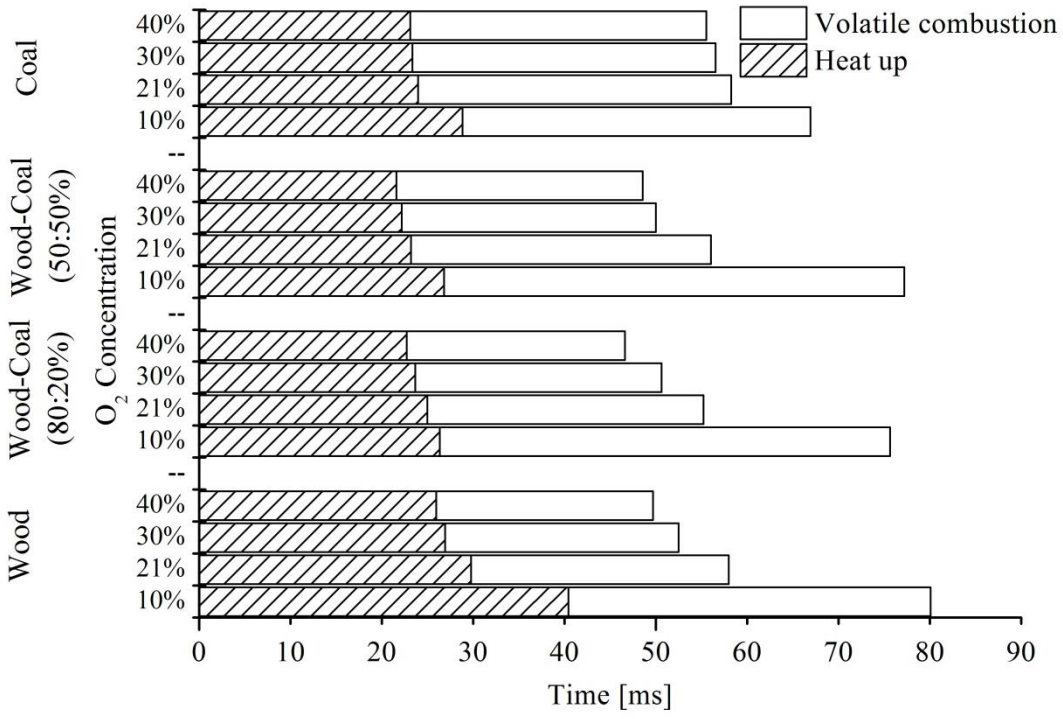

434

435 Fig. 10. Measurement of average duration of heat-up and volatile combustion, obtained from

four particles (255–300 μm) under different oxygen concentrations at 1,340 K. This figure shows different burning characteristics between the wood and coal particles and the two mixed particles.

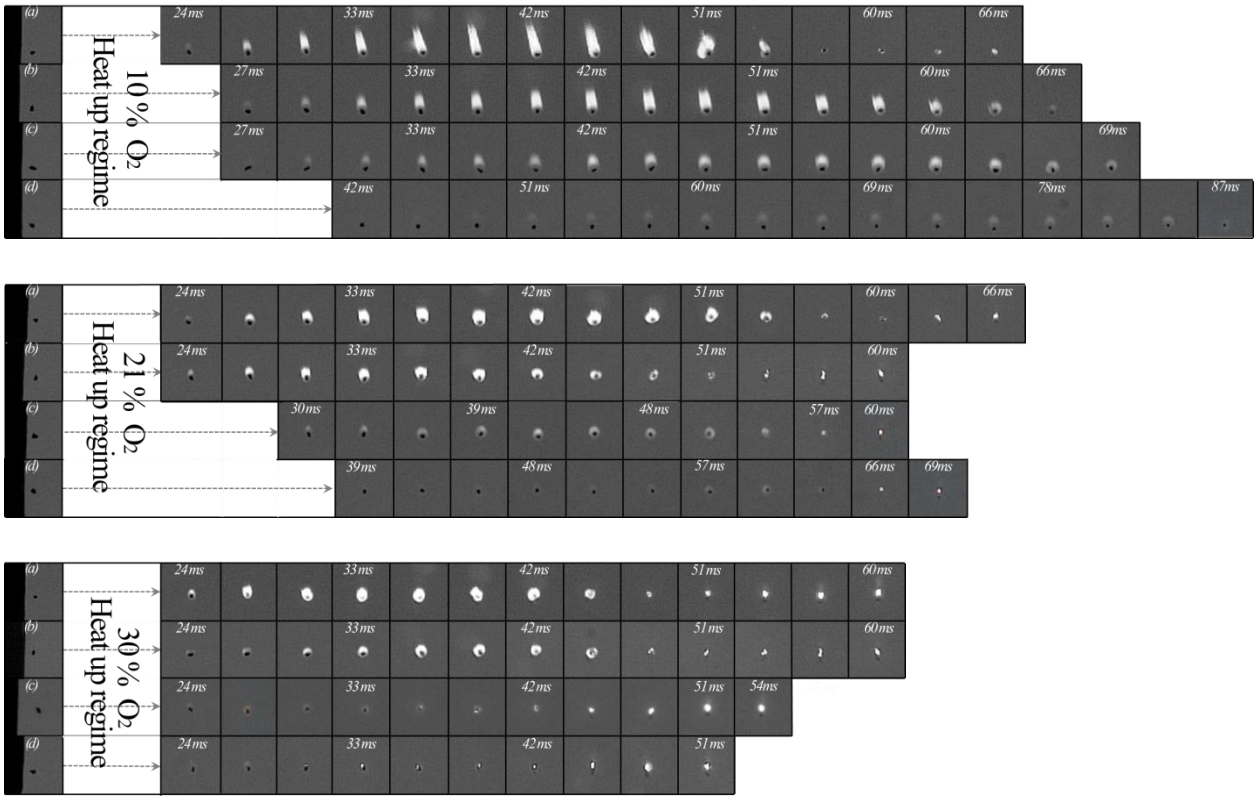

Fig. 11. Burning particles at 215–255 μm under 10%–30% O_2 concentrations at 1,340 K: (a) coal, (b) 20:80 coal/wood, (c) 50:50 coal/wood and (d) wood. The particles are captured over time intervals of 4 ms. The coal particle has the largest and brightest flame of the four.

3.4 Effect of particle types over time

The results shown in Fig. 12 suggest that increasing the coal blending ratio under 10 and 21% oxygen concentrations has a significant effect on the enveloped flame of each particle in the time domain. The size and intensity of the flames around particles (215-255 μm) were measured from volatile ignition to flame extinction. However, we cannot detect the whole

volatile combustion in particles (300-350 μm) as explained before. Particle combustion events are associated with a high peak when the maximum volume of volatiles and soot particles are in the flame. This can also be seen in the nearly symmetrical profile during combustion [17]. From this result, the profiles of the two particles with fuel mixtures are seen to lie between the coal and wood profiles. The peak flame size does not correspond entirely with the peak flame intensity, although they have similar tendencies over the same period. The peak of volatile flame area occurs marginally before the intensity peak.

Figure 13 shows the variation in maximum flame area and intensity under 21% O_2 at 1,340 K with the wood-coal blending ratio. The imagined line between wood and coal particles is drawn in order to compare their measured magnitudes. To obtain the results, the flame parameters were averaged over 20 particles for each test. The flame area of the 50:50 coal/wood particle differed from the prediction of the imagined line by 0.03 mm^2. Both the 20:80 and 50:50 coal/wood particles have a higher intensity compared with the trend in flame area. Also, there was little difference in intensity between the 50:50 coal/wood and pure coal particles under 21% O_2.

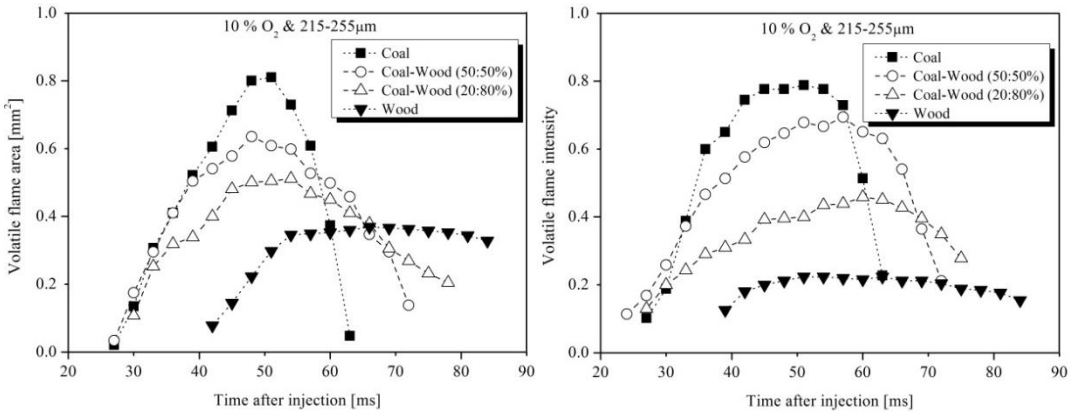

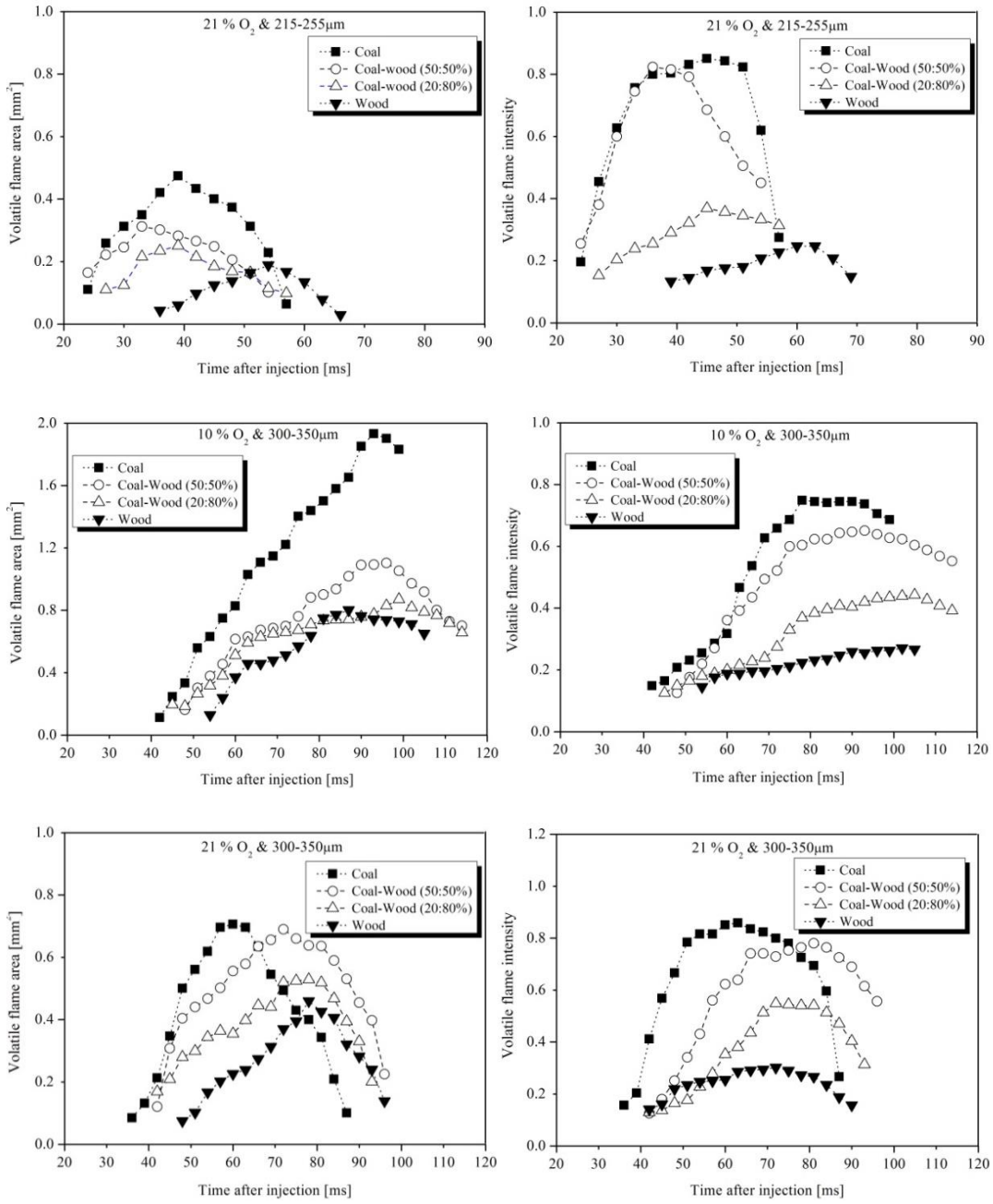

Fig. 12. Effect of particle type on flame development under 10 and 21% O_2 at 1,340 K. The figures show a peak in the flame parameters as a function of time, and distinguishable flame size and intensity between particles are measured at 215–255 μm and 300–350 μm.

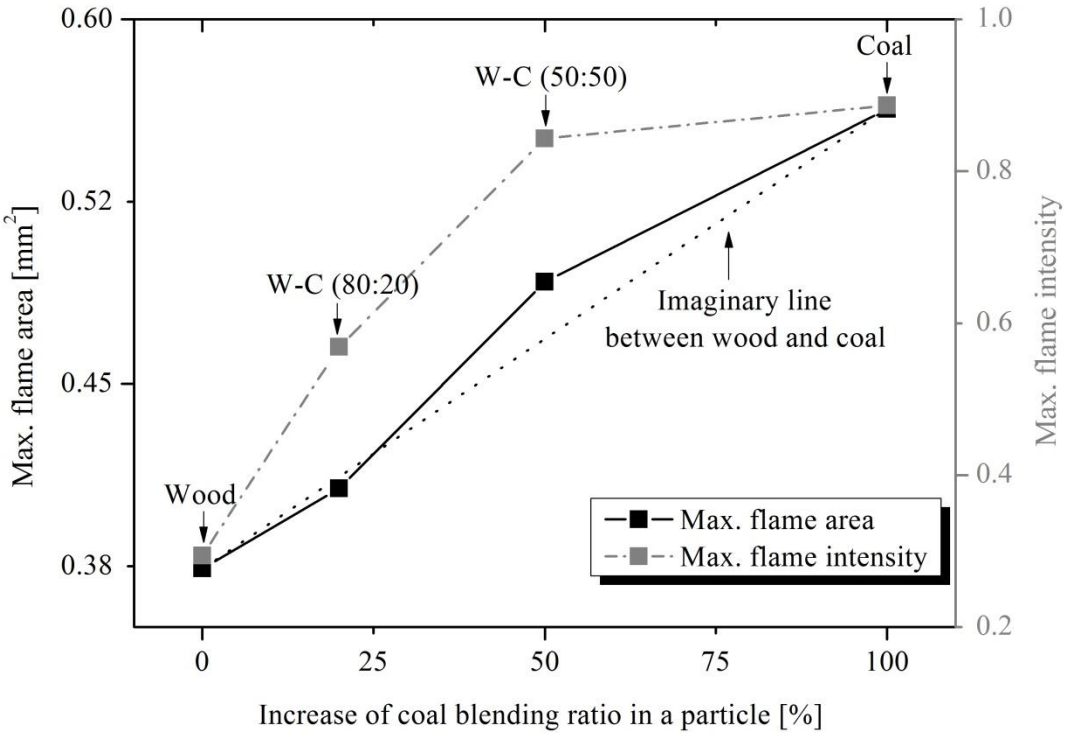

Fig. 13. Overall profiles of average flame parameters with particle coal-blending ratio (255–300 μm) under 21% O_2 at 1,340 K. This figure shows how flame intensity and area increase with reference to an imagined line between wood and coal.

3.5 Effect of oxygen concentration with particle type as a function of time

The four different types of particle in the particle size group of 215–255 μm were burned under 10%–40% O_2. Fig. 14 shows the temporal flame profiles for the effect of oxygen concentration. The flame area decreased with shorter volatile combustion time as the oxygen concentration was increased. A dramatic decrease of this flame parameter for particles at 255–300 μm was observed between 10 and 21 % oxygen, as shown in Fig. 15(a). Particles burning under low oxygen concentration have an elongated flame. The flame areas of coal, 50:50 coal/wood, 20:80 coal/wood and wood under 21%–30% O_2 decreased by approximately 44, 40, 59 and 79%, respectively. As for the combustion mode, particles

containing 80% or more of wood have imperceptible volatile flames with low luminosity at high oxygen concentrations, and simultaneous homogeneous and heterogeneous combustion occurs on the surface. Hence, coal blending plays an important role in stable flame structures and sequential combustion processes even under high oxygen concentrations.

Overall, the flame intensity of the four particles at 255–300 μm present the effect of oxygen concentration as shown in Fig. 15(b). The flame intensities on all the particles were comparatively high under 21% oxygen. However, the peak flame intensity of the coal particles was reached at 30% oxygen concentration, whereas the pure wood particle and particles with wood mixtures have their highest flame intensities at 21% O_2. This phenomenon is likely attributable to the volume fraction of soot in the flame. The normalised flame intensities of particles with high wood mixtures decreased dramatically between 21 % and 30 % O_2. Khatami et al. [15] reported that the highest peak soot volume fraction of bituminous coal occurred in 40 % O. The different profiles between two results are related to the particle size, environmental conditions and reaction rate.

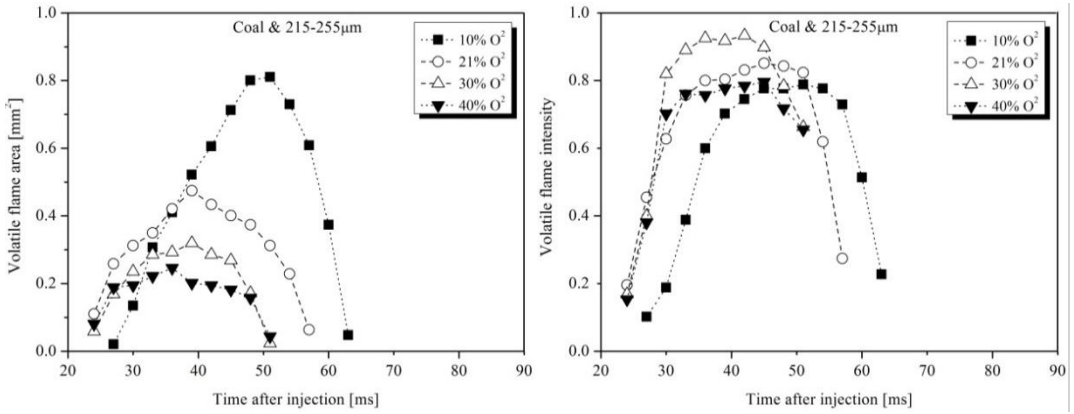

510

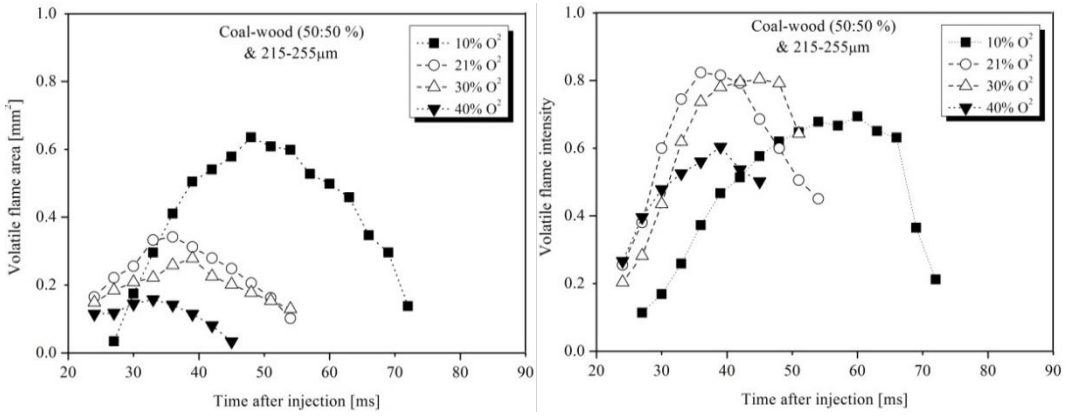

511

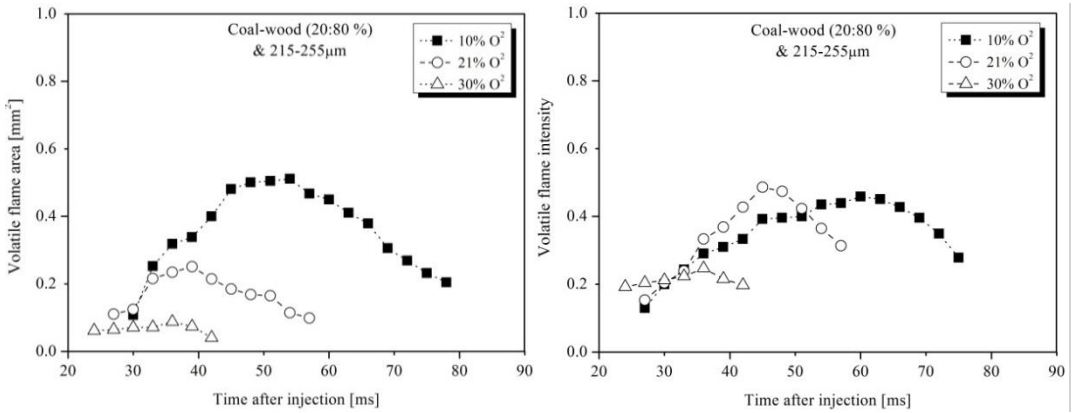

512

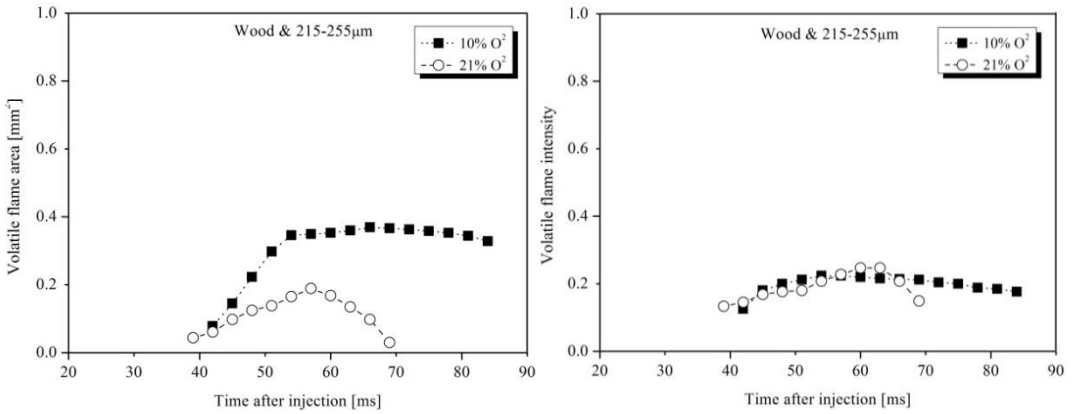

513

514 Fig. 14. Effect of oxygen concentration (10%–40%) on the flame characteristics of the four

particles (215–255 μm) at 1,340 K. The graphs illustrate the variation of volatile flame area and intensity with surrounding O_2.

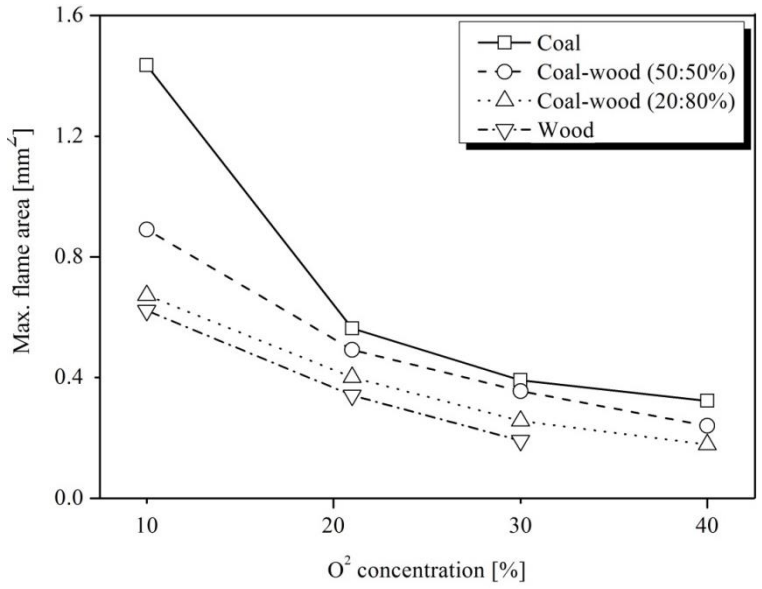

(a)

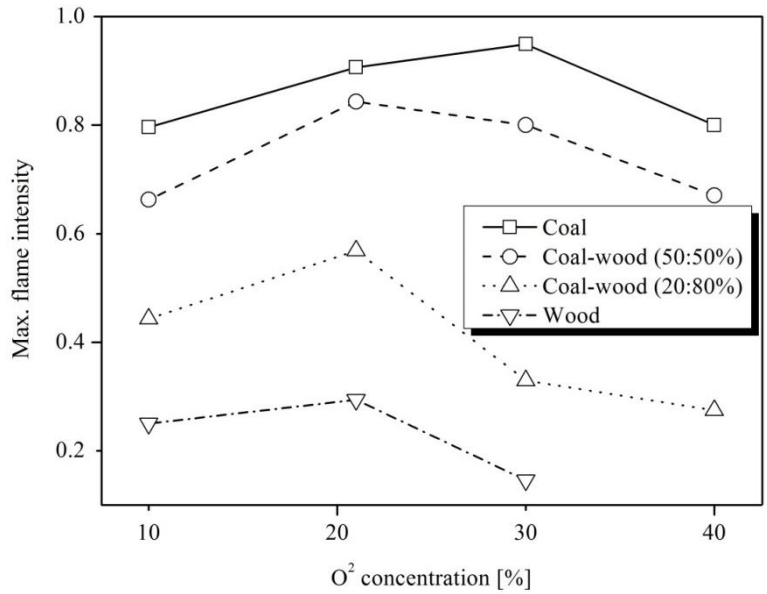

(b)

Fig. 15. Overall profiles of average flame area and intensity of the four particles (255–300 μm) with O_2 concentration. These graphs show a wide variation in flame area for the four particles under 10% O_2; wood and blended particles (not coal particles) have a peak flame intensity at 21% O_2.

3.6 Effect of particle size

Figure 16 shows superimposed visible flame appearances for particle sizes in the ranges of 215–255 μm and 300–350 μm. All the experiments were performed under 10% oxygen concentration at 1,340 K. After injection, the burning particles were captured at 4-ms time intervals. The increase of approximately 100 μm in the size of the four particle types clearly affected the ignition delay. The trajectories of the 300–350-μm particles dropped slightly after injection and then went upwards until burnout because of the relatively high particle mass. In the experiment, the particle size group of 355−425 μm dropped slightly after injection and then lifted toward the top until burnout. Larger particle sizes fall to the bottom to be incompletely burned without volatile combustion, which was explained by Mock et al. [17].

Figure 17 shows the average flame parameters for 20 particles of 215–255 μm and 300–350 μm under 21% oxygen concentration. This shows that the increase in flame size for all particles was very steady between the two particle-size groups. However, the increased flame intensity is a little different between coal particles and particles with a high coal-blending ratio. The coal and 50:50 coal/wood particles also show very similar flame intensity variations with particle size, which may be attributed to a sufficiently high soot particle volume fraction in the particles.

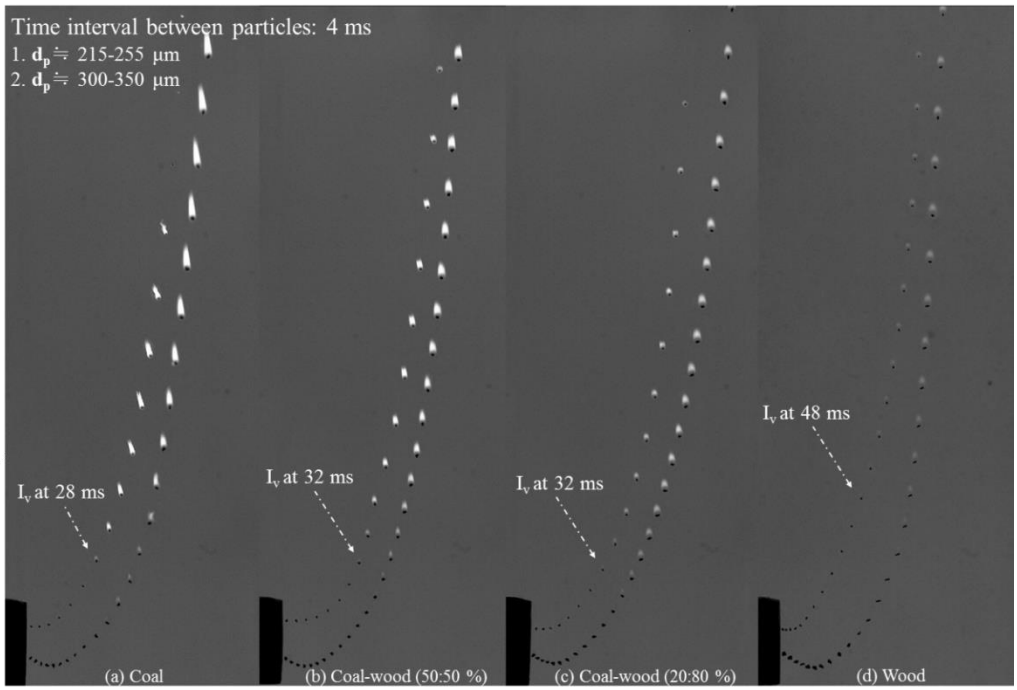

543

544 Fig. 16. Superposition of four different particles of 215–255 μm and 300–350 μm at time
545 intervals of 4 ms entrained in hot gas streams of 1,340 K under 10% oxygen concentration.
546 The tendencies of particles of different sizes are similar between the two particle size groups.
547 However, the flames on the 300–350 μm particles grow because of the longer ignition delay.

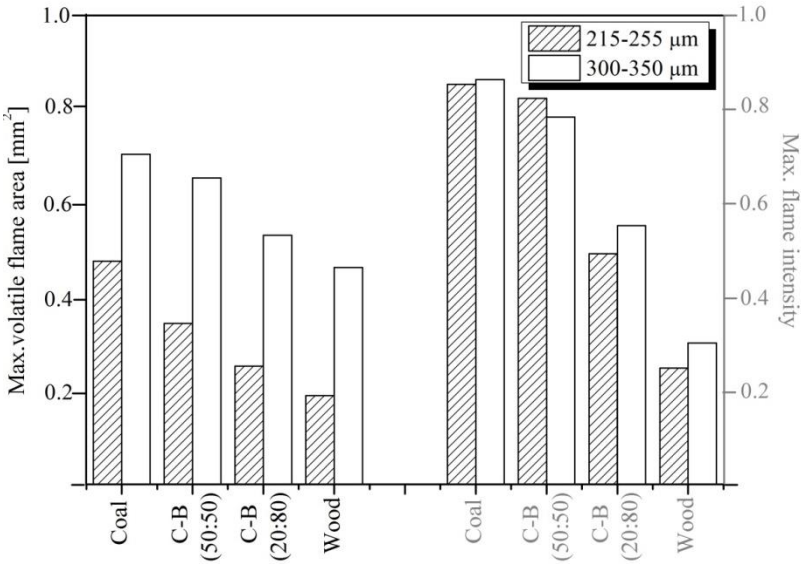

548

549 Fig. 17. Average flame area and intensity of four different particles with particle size (215–
550 255 μm and 300–350 μm) under 21% O_2 concentration. The graphs show a regular
551 decreasing trend in volatile flame area.

3.7 Flame aspect ratio of co-firing particles

The shapes of the flames on the four particle surfaces under 10 and 21% oxygen concentrations can be represented in terms of the flame aspect ratio. Figures 18(a) and (b) illustrate the measurement of flame height, length and intensity after image post-processing, which may be an effective way to define the characteristics of flame shape. One of the results is that a relatively large pyrolysis zone for fuel vaporisation and reactions was observed clearly under low oxygen concentration, showing a transparent coloured boundary layer. The flame aspect ratio increases rapidly for burning particles with a 50% coal blending ratio. However, wood and 20:80 coal/wood particle have aspect ratios of approximately 1.2, which suggests a more spherical flame. An elongated flame can be attributed to soot phase in a particle. Coal particles, which contain more fixed carbon and less volatile matter, have the highest visible flame aspect ratio of 3.4 under the lowest oxygen concentration.

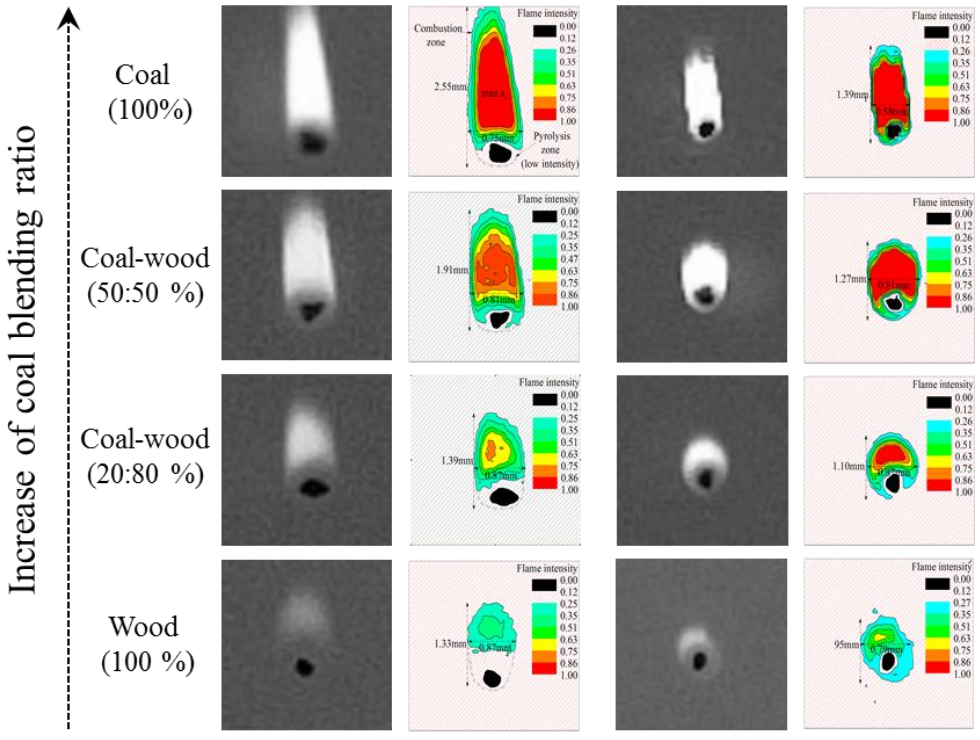

(a) 10 % O_2 (b) 21 % O_2

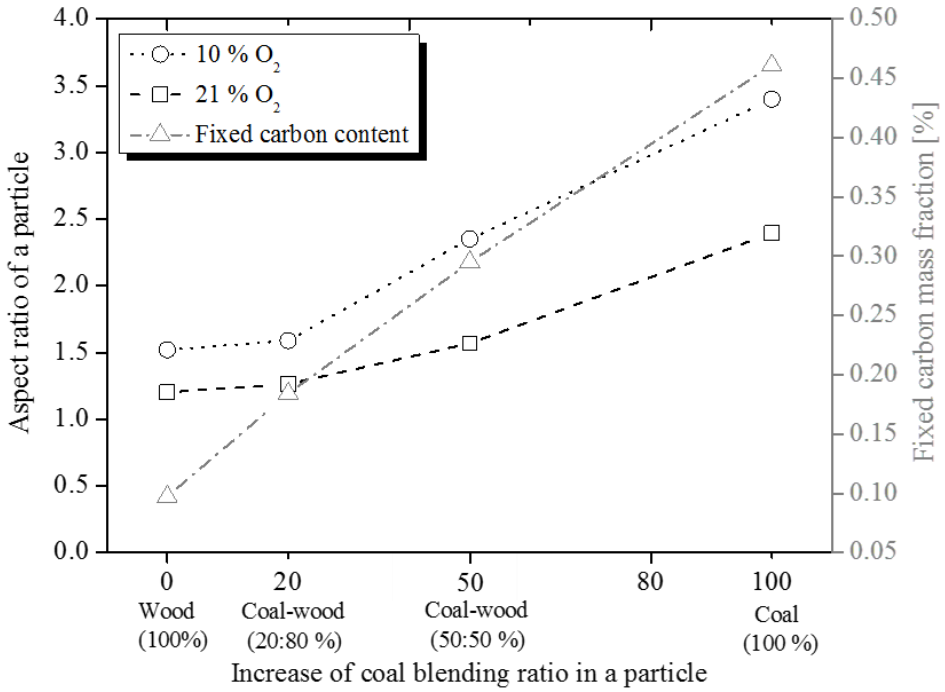

(c) Flame aspect ratio

Fig. 18. Flame structure in terms of aspect ratio obtained from volatile flames of four particles under 10 and 21% O_2 concentrations by image post-processing.

4. CONCLUSIONS

In the study, pulverised single solid-fuel particles with different fuel mixtures were burned in a lab-scale entrained-flow reactor. These were compared with the burning of pure coal and pure wood particles under identical environmental conditions. The four particles differed in relation to their chemical and physical characteristics, which in turn affected the flame characteristics. The main objectives were to assess the burning behaviours of mixed single particles for co-firing, focusing on ignition, flame area and intensity, and combustion time, from direct observation. Quantitative analysis of these combustion parameters was presented along with a description of the sequential combustion process of the particles under various oxygen concentrations and for different particle sizes. The burning of particles under both slow and rapid heating was also discussed in relation to the similarities and differences of

their combustion behaviours. The significant conclusions of this study are as follows:

1. Single particles were observed in sequential combustion processes such as heat-up, ignition and volatile and char combustion. Simultaneous volatile and char combustion has been observed in a particle with high wood mixture under enhanced oxygen concentrations.
2. The conical flame shape on co-firing particles was affected by an increase in the coal mixture ratio. This was because the high fixed carbon content and H/C ratio of coal generate a large soot flame with a high aspect ratio and flame intensity.
3. The pulverised particles are burned out in a few hundred milliseconds under rapid heating; coal particles ignited sooner than the apparent ignition of wood particles. As a result, the ignition of pulverised co-firing particles is attributed to the coal ignition characteristics. However, the volatile combustion time plays an important role in the high volatile matter content of the wood mixtures.
4. Of relevance to co-firing combustion is the fact that particles with coal/wood mixtures improve the radiative heat energy from the flame parameters compared with wood flames: +9% and +32% for the size and 93% and 187% for the intensity of 20:80 coal/wood and 50:50 coal/wood, respectively, under 21% O_2. This may affect the stable diffusion flame, the fast homogeneous ignition and the flame stability to the boiler efficiency.

Acknowledgments

The authors gratefully acknowledge the support of the Korea Advanced Institute of Science and Technology (KAIST) and the Brain Korea 21+ project. Also, this work was supported by the "R&D Program for Convergence Technology between National Institutes", funded by the Korea Institute of Industrial Technology grant (EO160063). Furthermore, we also thank Jae Young Yoo (KAIST postgraduate student), Dr Myung Won Seo and Dr Ho Won Ra (the Korea Institute of Energy Research), who actively contributed to the sample preparation.

References

[1] Sondreal, E. A., S. A. Benson, J. P. Hurley, M. D. Mann, J. H. Pavlish, M. L. Swanson, G. F. Weber and C. J. Zygarlicke (2001). "Review of advances in combustion technology and biomass cofiring." Fuel Processing Technology 71(1): 7-38.

[2] Sahu, S., N. Chakraborty and P. Sarkar (2014). "Coal–biomass co-combustion: an overview." Renewable and Sustainable Energy Reviews 39: 575-586.

[3] Spliethoff, H. and K. Hein (1998). "Effect of co-combustion of biomass on emissions in pulverized fuel furnaces." Fuel processing technology 54(1): 189-205.

[4] Tillman, D. A. (2000). Cofiring benefits for coal and biomass, Pergamon.

[5] Sweeten, J. M., K. Annamalai, B. Thien and L. A. McDonald (2003). "Co-firing of coal and cattle feedlot biomass (FB) fuels. Part I. Feedlot biomass (cattle manure) fuel quality and characteristics." Fuel 82(10): 1167-1182.

[6] Hein, K. and J. Bemtgen (1998). "EU clean coal technology—co-combustion of coal and biomass." Fuel processing technology 54(1): 159-169.

[7] Baxter, L. (2005). "Biomass-coal co-combustion: opportunity for affordable renewable energy." Fuel 84(10): 1295-1302.

[8] Wieck-Hansen, K., P. Overgaard and O. H. Larsen (2000). "Cofiring coal and straw in a 150 MW e power boiler experiences." Biomass and bioenergy 19(6): 395-409.

[9] Demirbas, A. (2004). "Combustion characteristics of different biomass fuels." Progress in energy and combustion science 30(2): 219-230.

[10] Koppejan, J. and S. Van Loo (2012). The handbook of biomass combustion and co-firing, Routledge.

[11] Pronobis, M. (2006). "The influence of biomass co-combustion on boiler fouling and efficiency." Fuel 85(4): 474-480.

[12] Mun, T.-Y., T. Z. Tumsa, U. Lee and W. Yang (2016). "Performance evaluation of co-firing various kinds of biomass with low rank coals in a 500 MWe coal-fired power plant." Energy 115: 954-962.

[13] Li, J., M. C. Paul, P. L. Younger, I. Watson, M. Hossain and S. Welch (2016). "Prediction of high-temperature rapid combustion behaviour of woody biomass particles." Fuel 165: 205-214.

[14] Li, J., M. C. Paul, P. L. Younger, I. Watson, M. Hossain and S. Welch (2015). "Characterization of biomass combustion at high temperatures based on an upgraded single particle model." Applied Energy 156: 749-755.

[15] Khatami, R., Y. A. Levendis and M. A. Delichatsios (2015). "Soot loading, temperature and size of single coal particle envelope flames in conventional-and oxy-combustion conditions (O 2/N 2 and O 2/CO 2)." Combustion and Flame 162(6): 2508-2517.

[16] Gil, M. V., D. Casal, C. Pevida, J. Pis and F. Rubiera (2010). "Thermal behaviour and kinetics of coal/biomass blends during co-combustion." Bioresource Technology 101(14): 5601-5608

[17] Mock, C., H. Lee, S. Choi and V. Manovic (2016). "Combustion Behavior of Relatively Large Pulverized Biomass Particles at Rapid Heating Rates." Energy & Fuels.

[18] Ahn, S., G. Choi and D. Kim (2014). "The effect of wood biomass blending with pulverized coal on combustion characteristics under oxy-fuel condition." Biomass and Bioenergy 71: 144-154.

[19] Wang, G., J. Zhang, J. Shao, Z. Liu, G. Zhang, T. Xu, J. Guo, H. Wang, R. Xu and H. Lin (2016). "Thermal behavior and kinetic analysis of co-combustion of waste biomass/low rank coal blends." Energy Conversion and Management 124: 414-426.

[20] Zhou, C., G. Liu, X. Wang and C. Qi (2016). "Co-combustion of bituminous coal and

biomass fuel blends: Thermochemical characterization, potential utilization and environmental advantage." Bioresource Technology 218: 418-427.
[21] Sarofim, A. and H. Hottel (1978). Radiative transfer in combustion chambers: influence of alternative fuels. Proceedings of the Sixth International Heat Transfer Conference.
[22] Mengüç, M., S. Manickavasagam and D. D'sa (1994). "Determination of radiative properties of pulverized coal particles from experiments." Fuel 73(4): 613-625.
[23] Atiku, F. A., E. J. S. Mitchell, A. R. Lea-Langton, J. M. Jones, A. Williams and K. D. Bartle (2016). "The Impact of Fuel Properties on the Composition of Soot Produced by the Combustion of Residential Solid Fuels in a Domestic Stove." Fuel Processing Technology 151: 117-125.
[24] Miedema, J. H., R. M. Benders, H. C. Moll and F. Pierie (2017). "Renew, reduce or become more efficient? The climate contribution of biomass co-combustion in a coal-fired power plant." Applied Energy 187: 873-885.
[25] Biagini, E., F. Lippi, L. Petarca and L. Tognotti (2002). "Devolatilization rate of biomasses and coal–biomass blends: an experimental investigation." Fuel 81(8): 1041-1050.
[26] Gani, A., K. Morishita, K. Nishikawa and I. Naruse (2005). "Characteristics of co-combustion of low-rank coal with biomass." Energy & Fuels 19(4): 1652-1659.
[27] Lu, G., Y. Yan, S. Cornwell, M. Whitehouse and G. Riley (2008). "Impact of co-firing coal and biomass on flame characteristics and stability." Fuel 87(7): 1133-1140.
[28] Molcan, P., G. Lu, T. Le Bris, Y. Yan, B. Taupin and S. Caillat (2009). "Characterisation of biomass and coal co-firing on a 3MWth combustion test facility using flame imaging and gas/ash sampling techniques." Fuel 88(12): 2328-2334.
[29] Lee, H. and S. Choi (2015). "An observation of combustion behavior of a single coal particle entrained into hot gas flow." Combustion and Flame 162(6): 2610-2620.
[30] Levendis, Y. A., K. Joshi, R. Khatami and A. F. Sarofim (2011). "Combustion behavior in air of single particles from three different coal ranks and from sugarcane bagasse." Combustion and Flame 158(3): 452-465.
[31] Khatami, R., C. Stivers and Y. A. Levendis (2012). "Ignition characteristics of single coal particles from three different ranks in O 2/N 2 and O 2/CO 2 atmospheres." Combustion and Flame 159(12): 3554-3568.
[32] Riaza, J., R. Khatami, Y. A. Levendis, L. Álvarez, M. V. Gil, C. Pevida, F. Rubiera and J. J. Pis (2014). "Combustion of single biomass particles in air and in oxy-fuel conditions." Biomass and Bioenergy 64: 162-174.
[33] Lee, H. and S. Choi (2016). "Motion of single pulverized coal particles in a hot gas flow field." Combustion and Flame 169: 63-71.
[34] Tyler, R. J. (1980). "Flash pyrolysis of coals. Devolatilization of bituminous coals in a small fluidized-bed reactor." Fuel 59(4): 218-226.
[35] Niazmand, H. and M. Renksizbulut (2003). "Transient three-dimensional heat transfer from rotating spheres with surface blowing." Chemical Engineering Science 58(15): 3535-3554.
[36] Mitchell, E., A. Lea-Langton, J. Jones, A. Williams, P. Layden and R. Johnson (2016). "The impact of fuel properties on the emissions from the combustion of biomass and other solid fuels in a fixed bed domestic stove." Fuel Processing Technology 142: 115-123.
[37] Shaddix, C. R. and A. Molina (2009). "Particle imaging of ignition and devolatilization of pulverized coal during oxy-fuel combustion." Proceedings of the Combustion Institute 32(2): 2091-2098.
[38] McLean, W., D. Hardesty and J. Pohl (1981). Direct observations of devolatilizing pulverized coal particles in a combustion environment. Symposium (International) on Combustion, Elsevier.

[39] Fletcher, T. H., J. Ma, J. R. Rigby, A. L. Brown and B. W. Webb (1997). "Soot in coal combustion systems." Progress in Energy and Combustion Science 23(3): 283-301.
[40] Khatami, R., C. Stivers, K. Joshi, Y. A. Levendis and A. F. Sarofim (2012). "Combustion behavior of single particles from three different coal ranks and from sugar cane bagasse in O 2/N 2 and O 2/CO 2 atmospheres." Combustion and flame 159(3): 1253-1271.
[41] Stanmore, B., Y.-C. Choi, R. Gadiou, O. Charon and P. Gilot (2000). "Pulverised coal combustion under transient cloud conditions in a drop tube furnace." Combustion science and technology 159(1): 237-253.
[42] Yang, H., R. Yan, H. Chen, D. H. Lee and C. Zheng (2007). "Characteristics of hemicellulose, cellulose and lignin pyrolysis." Fuel **86**(12): 1781-1788.
[43] Trubetskaya, A., P. A. Jensen, A. D. Jensen, A. D. G. Llamas, K. Umeki, D. Gardini, J. Kling, R. B. Bates and P. Glarborg (2016). "Effects of several types of biomass fuels on the yield, nanostructure and reactivity of soot from fast pyrolysis at high temperatures." Applied Energy **171**: 468-482.
[44] Septien, S., S. Valin, M. Peyrot, C. Dupont and S. Salvador (2014). "Characterization of char and soot from millimetric wood particles pyrolysis in a drop tube reactor between 800 C and 1400 C." Fuel **121**: 216-224.